Biochimica et Biophysica Acta, 946 (1988) 165–172
Elsevier

BBA 70584

BBA Report

First direct observation of the water exchange across the membrane of a single-cell green alga on a cellular level

Rüdiger Lawaczeck

Institute of Physical Chemistry, University of Würzburg, Würzburg (F.R.G.)

(Received 8 July 1988)

Key words: Water exchange; Membrane permeability; Isotope exchange; Infrared microscopy; Near infrared image; Isotope absorption difference spectroscopy; (Alga)

The isotopic water exchange across the membrane of a single-cell alga is made visible by optical differences of H_2O and ^2H_2O. In the near infrared (NIR) (1000 to 2500 nm) H_2O shows pronounced absorption bands while ^2H_2O is almost transparent. Results from in vivo experiments on the diffusive water permeation across the membrane of the spherical freshwater alga *Eremosphaera viridis* are presented. The evaluation of the isotope-exchange kinetics allows the calculation of the permeability coefficient, P_d, and the approximation of the intracellular diffusion constant, D. The extension of $H_2O/^2H_2O$-exchange measurements to two dimensions opens new ways to study transport pathways up to the spatial resolution of a microscope. First NIR video images demonstrate the capability of the method.

Introduction. Light microscopy, including video enhancement techniques [1], is becoming a widespread tool for the observation of cellular processes. It is presently possible to do quantitative spectroscopy on micrometer-spots, i.e. less the size of erythrocytes, with significant wavelength resolution at a high repetition rate (one spectrum in 15 ms (Lawaczeck, to be published)). However, the visualization of the flow of water and of most electrolytes lacks behind. Only a few ion-specific probes [2,3] are available for the direct observation of ion transports. The visible observations were recently complemented by micro NMR-images of water from single cells [4].

Water plays an essential role for all living organisms. Thus it is desirable to look at the permeation and diffusion of water down to cellular dimensions. In the following a strategy together with first results will be described for the direct observation of the water exchange across membranes of single cells. The studies performed rely on the isotope absorption difference spectroscopy (IADS) in the near infrared (NIR) [5]. The method has so far been explored to study the water exchange in thin tissues and plant leaves in situ [5]. Here first in vivo measurements of the isotopic water-exchange will be reported with the spatial resolution of the light microscope and a time-resolution in the ms range. This time-scale is only limited by the mixing of normal and deuterated buffer. Results on the water permeation across the membrane of the single-cell freshwater alga *Eremosphaera viridis* will be presented. The evaluation of the data further allows the approximate calculation of the intracellular diffusion of water. The extension of the permeability measurements to two-dimensional images offers new perspectives to study transport phenomena. First

Correspondence: R. Lawaczeck, Diagnostics Research Institute, c/o Free University of Berlin, Spandauer Damm 130 No. 9, D-1000 Berlin 19, Germany.

results on this line by a NIR video technique have been obtained. The direct visualization of the water flow or exchange is especially helpful for the understanding of permeation pathways in organized systems where – depending on the height of the barriers – water can use trans- and/or extracellular pathways. On the basis of image processing devices $H_2O/^2H_2O$-difference maps can further be produced at various time intervals.

Measuring principle. The method to follow the $H_2O/^2H_2O$ exchange is based on the difference of the absorption of H_2O and ^2H_2O in the near infrared (NIR), i.e. in the spectral region from about 1000 to 2500 nm. Representative NIR spectra of H_2O and ^2H_2O are redrawn in Fig. 1. H_2O shows a pronounced absorption while ^2H_2O is practically transparent in that spectral region. The absorption lines are due to overtones and combinations of the fundamental IR vibration modes and may further serve as fingerprints of the water structure [6]. For experimental reasons (availability of sensitive detectors and vidicons) we have focussed on the prominent absorption difference of H_2O and ^2H_2O at 1450 nm. From the absorption at 1450 nm the $H_2O/^2H_2O$ exchange-kinetics can be monitored in situ by recording the intracellular NIR absorption while an isotope change of the extracellular solvent (e.g. H_2O vs. ^2H_2O) is performed. In previous measurements on plant leaves, fibre optics were used with an observation area in the range of 5 mm^2. The present studies were performed in a transmission microscope spectrometer allowing to scale down the observation area to the μm^2 range so that the transmitted light from intracellular areas can be recorded.

Material and Methods. The algae *Eremosphaera viridis* were grown in Mes (4-morpholineethanesulfonic acid) or phosphate buffer at pH 5.6 by Dr. K. Köhler at the Institute of Botany, University of Würzburg [7]. The algae had an average diameter of 150 μm.

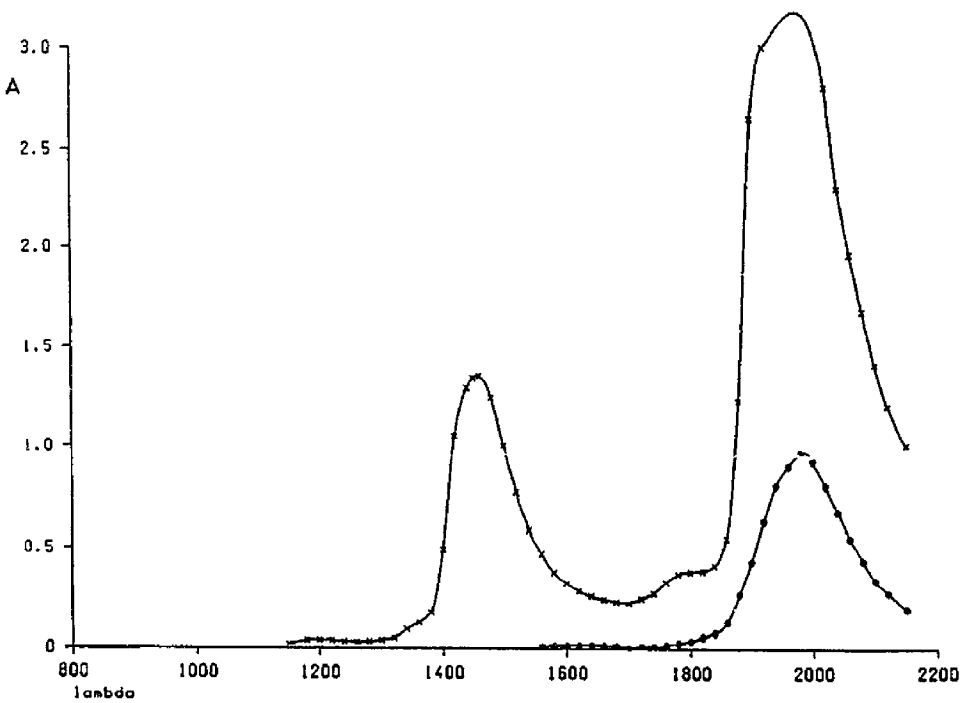

Fig. 1. Near infrared (NIR) spectra of H_2O (×) and ^2H_2O (○). Absorbance vs. wavelength in nm, cuvette length 1 mm, room temperature, neutral pH (p^2H).

Inorganic chemicals at highest available purity and deuterium oxide, ^2H_2O, were obtained from E. Merck, Darmstadt. The deuterated buffer was prepared by lyophilisation of the normal buffer and resolubilization in ^2H_2O. The algae were fixed with thin cotton filaments between glass support and cover slide on the stage of the Zeiss UEM microscope working in transmission mode. The microscope was equipped with a spectrometer accessory allowing quantitative measurements of light intensities from small observation areas. The size of these areas depends on the magnification chosen. The present experiments were performed with neofluar objectives with either 10- or 25-fold magnification. Either a Zeiss XBO 75 W or a halogen 100 W lamp served to illuminate the probes; both light sources extend into the near infrared region. A NIR narrow-band interference filter (Oriel, Darmstadt) was placed in front of the condensor lens so that only light at 1450 nm passed into the cell. Measurements on plant leaves had revealed that light at this wavelength is harmless in contrast to light at the fundamental water absorption in the IR. No temperature changes could be measured by directing the NIR-light on a thermocouple. For quantitative measurements the light was chopped at variable frequencies in order to compensate small drifts of the dark current. The transmitted NIR light was detected by a Peltier-cooled NIR-sensitive detector (PbS photoconductive cells P1026, Hamamatsu). The resultant signals were stored in a transient recorder (Krenz Electronics, Hirzenhain) connected to a microcomputer. A soft-ware program demodulated the signals and displayed the averaged differences between the on/off positions of the light chopper. Usually 32K data points at 12 bit resolution were measured for one experiment. The isotope exchange of the buffer was performed by carefully sucking the new buffer through the small gap between glass support and cover slide.

For some experiments a NIR-sensitive camera system (Hamamatsu microscope video camera C2400 with infra-red vidicon) was connected to the microscope allowing the direct visualization of the $H_2O/^2H_2O$-exchange on the video monitor.

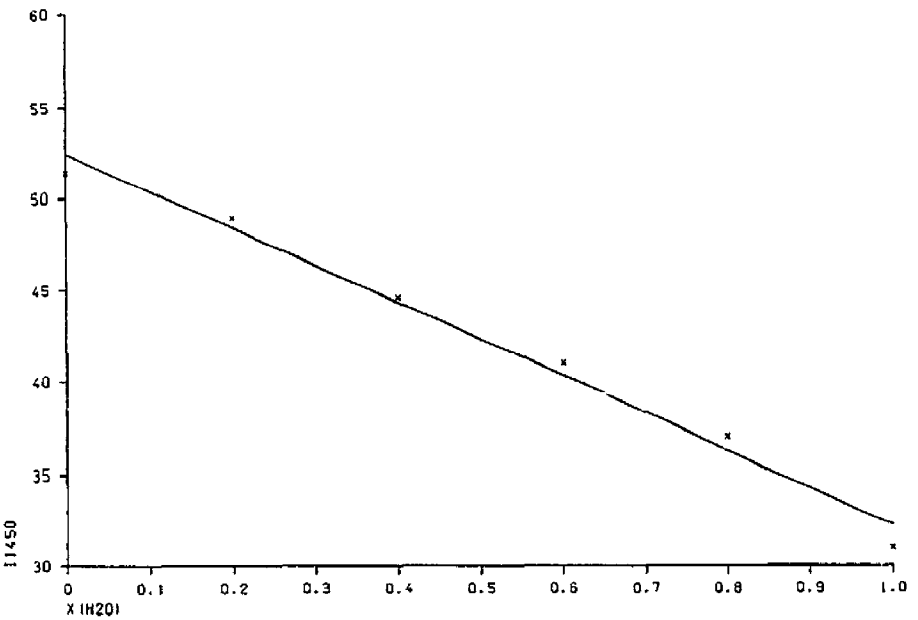

Fig. 2. Intensity of the transmitted light (I_{1450}) through the microscope-spectrometer vs. the stoichiometric mole fraction of H_2O ($x(H_2O)$) of layers, 0.15 mm thick. The straight line drawn (by a linear least-squares fit) is an approximation of the curvilinear behaviour.

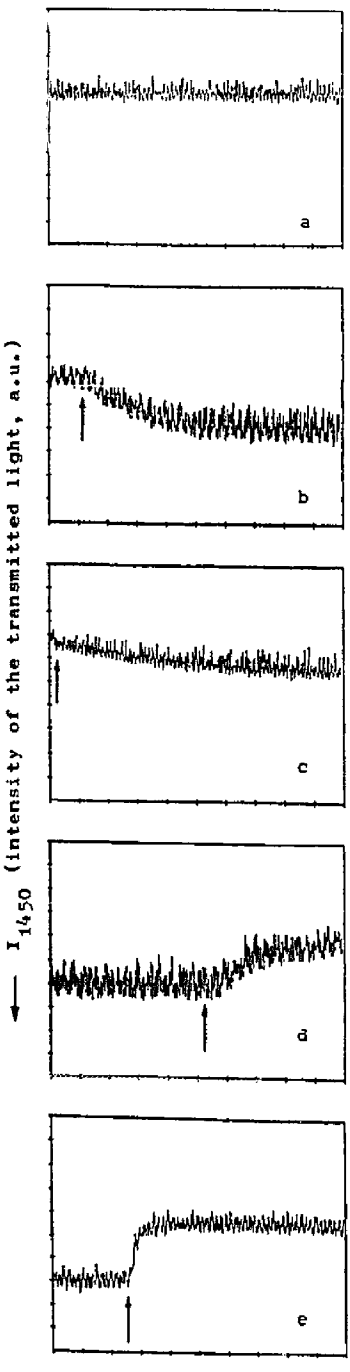

These studies revealed that the algae remained in the focal plane in about 80% of the mixing experiments.

Results and Discussion. The microscopic observation system of the $H_2O/^2H_2O$ exchange was calibrated in stationary experiments. For that purpose thin layers (thickness 0.15 mm) of $H_2O/^2H_2O$ mixtures were placed in the focal plane. The measured intensities of the transmitted light as function of the $H_2O/^2H_2O$ composition are shown in Fig. 2. The small deviation from linearity is expected on the basis of the minor H^2HO-contribution to the absorption at 1450 nm [8] and can be tolerated. Spectra (1000–1750 nm, with NIR monochromators) from these thin layers pointed to pronounced $H_2O/^2H_2O$ differences at 1450 nm qualitatively reflecting the isotope behaviour of Fig. 1, though these (single beam) intensities contained the wavelength dependence of the total microscope system (light source, prism-monochromator, optics, detector). Thus any changes of the transmitted light at 1450 nm are directly correlated with the $H_2O/^2H_2O$ content in the observation area.

Fig. 3 summarizes results of experiments with *Eremosphaera viridis* using an observation spot of 35 μm diameter. The transmitted light at 1450 nm from the 35-μm spots outside or inside the spherical algae of 150 μm diameter are plotted as function of the time. The data storage was started before the solvent change. For some experiments the cells were centrifuged for short times which led to a separation of the intracellular compartments. One can thus distinguish between cytoplasm plus chloroplasts and vacuole without destroying the cell integrity (the vacuole fills about 75% of the intracellular volume; Köhler, K. private

Fig. 3. A series of $H_2O/^2H_2O$-exchange experiments. Intensity of the transmitted light (a.u., upwards decreasing) at 1450 nm vs. time. Maximal observation time is 16 s. The alga was fixed between glass support and cover slide while the isotope-exchanges of the solvent, indicated by arrows, were performed. Observation spot 35 μm. The isotope-changes are (from top to bottom); (a) H_2O vs. H_2O (control); (b and c) ^2H_2O vs. H_2O; (d and e) H_2O vs. ^2H_2O. (c) refers to a normal cell, b and d to centrifuged cells, respectively. (e) measures the solvent flux through the observation area of 35 μm diameter just outside the cell.

communication). From top to bottom the experiments in Fig. 3 refer to the mixing of H_2O/H_2O (control), $H_2O/^2H_2O$, $H_2O/^2H_2O$, $^2H_2O/H_2O$, and $^2H_2O/H_2O$, respectively. In Fig. 3e the observation spot was placed outside the cell; thus the signal showed the mathematically expected sigmoidal (for spherical observation areas) shape allowing the determination of the flow rate. In Fig. 3c a normal and in Figs. 3b and 3d centrifuged cells, were observed, respectively.

The water permeation across biological membranes (diffusive and osmotically driven) is extensively studied [9,10] with a great number of investigations devoted to the red cell membrane (see, for example, Ref. 11). So far most of the studies on the water permeation are concerned with systems where the plasmamembrane or the lipid bilayer separates two aqueous compartments. The permeability coefficients, P_d, are calculated from life-times or exchange relaxation times, τ_{ex}, within the intracellular compartment at known volume to surface ratio, V/S, according to

$$\tau_{ex} = V/(S \cdot P_d) \qquad (1)$$

For spherical cells like the *Eremosphaera viridis* with radius, r, τ_{ex} is simply given by $r/(3\,P_d)$. In the present case several barriers in series have to be considered, i.e. the external unstirred layer, the cell wall, the plasmalemma and the vacuole membrane. Furthermore the intracellular mixing might be hindered by intracellular organelles. Far reaching external unstirred layers can certainly be excluded due to the miniaturization of the experimental observation. For *Eremosphaera viridis* the removal of the cell wall leading to intact protoplasts was so far not successful (Ref. 12, and Köhler, K. private communication). The cell wall is 0.7 μm thick and has a fibril structure [12]. However, the cell wall should only slow down the permeation process if the diffusion constant within the cell wall is rather small and pores are absent. Usually the barrier built up by cell walls is not considered as rate-limiting for the transfer of small molecules (including ions). In a first approximation the exchange relaxation times, τ_{ex}, were obtained by a monoexponential fit of the time-dependent transmission intensity, I_t, from Fig. 3 according to

$$I_t = A_1 \cdot \exp(-t/\tau_{ex}) + A_2 \qquad (2)$$

where the A_i values are constants.

Table I shows the values of τ_{ex} and P_d for the two cases, normal cells with intracellular organelles within the cytosol and centrifuged cells with the organelles at one side of the cell only. The flux through the observation window (35 μm diameter) was $2.1 \cdot 10^{-3}$ cm/s. Major effects due to differences of the self-diffusion coefficients for H_2O and ^2H_2O were not observed (the diffusion of ^2H_2O is about 16% slower than that of H_2O [13]).

For small cells up to the size of mammalian erythrocytes the permeation step is rate-determining and the intracellular mixing times can be neglected [11]. In the present case the intracellular mixing/diffusion might well contribute to the observed time course. Using equations derived by Crank [14] for the effect of internal diffusion and evaporation, one can approximate the influence of the intracellular diffusion on the permeation rates observed. Lövtrup [15] has considered the diffusion within and the water exchange across animal cells, this case is comparable to the present measurements. He arrived at the following estimates of the time-dependence for exchange-type experiments:

$$\frac{I_t - I_\infty}{I_0 - I_\infty} = \frac{6L^2 \cdot \exp(-\beta^2 Dt/r^2)}{\beta^2[\beta^2 + L(L-1)]} \qquad (3)$$

with $L = r \cdot P_d/D$ and β given by the solution of Eqn. 4.

$$\beta = (1 - L) \cdot \tan\beta \qquad (4)$$

D is the intracellular diffusion coefficient; I_t, I_0 and I_∞ are the signal intensities (proportional to the $H_2O/^2H_2O$ content for thin layers) at time t,

TABLE I

	Normal cell	Free cytosol
Exchange time, τ_{ex}	8.62 s	2.87 s
Permeability coefficient, P_d	$2.9 \cdot 10^{-4}$ cm/s	$8.7 \cdot 10^{-4}$ cm/s

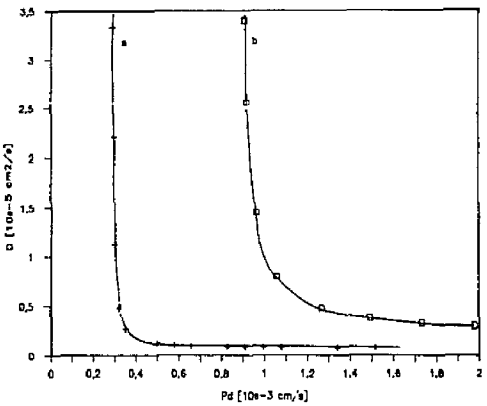

Fig. 4. Influence of the intracellular mixing by diffusion on the observed exchange time, τ_{ex}. Intracellular diffusion coefficient, D, vs. permeability coefficient, P_d, compatible with the experimental results ($\tau_{ex} = 8.62$ and 2.87 s, respectively). The cells were treated as hollow spheres with a radius of 75 μm (volume to surface ratio = 25 μm). The curves drawn refer to the normal (a, (+)) and centrifuged (b, (□)) cells. For a diffusion coefficient of $4.5 \cdot 10^{-6}$ cm^2/s of the free intracellular space (centrifuged cells) the permeability coefficient is $1.25 \cdot 10^{-3}$ cm/s leading to a diffusion coefficient of $1 \cdot 10^{-6}$ cm^2/s for the chloroplast-filled cytosol (normal cells).

0 (before the mixing) and infinity, respectively. Eqn. 1 is no longer valid and is substituted by

$$\tau_{ex} = r^2/(D \cdot \beta^2) \qquad (5)$$

For low values of L ($L \ll 1$) Eqn. 5 approaches Eqn. 1. Low values of L correspond to small cellular radii and/or small P_d/D ratios. For the latter case the permeation step is rate-limiting. At known relaxation time, τ_{ex}, and cellular radius, r, the permeability coefficient, P_d, and the diffusion constant, D, are related by the Eqns. 4 and 5. D vs. P_d curves were constructed in Fig. 4. The two curves indicated are compatible with the cellular radius of 75 μm and with results of the exponential fit of the curves in Fig. 3. For each of these two τ_{ex} values D is chosen and β calculated on the basis of Eqn. 5. This β is inserted into Eqn. 4 and the corresponding L and consequently P_d were obtained either by a graphical or by an iterative solution. Curves analogous to Fig. 4 have been considered earlier [16,17] for a general discussion of the relation between P_d, D and the observable exchange relaxation time τ_{ex}. From the two curves in Fig. 4 calculated for the normal and particle-free system it is evident that the P_d values become equal if the diffusion coefficients in the free and chloroplasts containing cytosol are different with $D_{\text{free cytosol}} > D_{\text{normal}}$.

The permeation across both the cell wall and the membranes should not be affected by the centrifugation of the cells therefore the P_d values should be equal for the two cases considered. Fig. 4 reveals that a common P_d is only possible for small D values with $D_{\text{free cytosol}} \leq 1 \cdot 10^{-5}$ cm^2/s and $D_{\text{normal}} \leq 2 \cdot 10^{-6}$ cm^2/s. On the other hand for the P_d values an opposite limit holds with $P_d \geq 1 \cdot 10^{-3}$ cm/s. Compared with the free self-diffusion a reduction of the intracellular diffusion seems reasonable since chloroplasts or other intracellular particles should increase the resistance to diffusion and therefore the times for the intracellular mixing as is experimentally observed in Fig. 3. Reported values for $D_{\text{intracellular}}$ are in the order of $1 \cdot 10^{-6}$ to $1 \cdot 10^{-5}$ cm^2/s [18,19]. Within these values for the intracellular diffusion an upper limit of P_d would be around $2 \cdot 10^{-3}$ cm/s. The limits for the P_d-coefficients ($1 \cdot 10^{-3} \leq P_d \leq 2 \cdot 10^{-3}$ in cm/s) fall well into the range determined for the diffusional water permeation across membranes from plant [20–22] and animal cells [11,23,24] and even for the water permeation across lipid bilayers in the fluid state [11,25]. The similarity of these values argues against a major contribution of the cell wall to the permeation barrier. As observed for the permeation across membranes from other cells the osmotic permeability coefficient, P_f, for the algae *Eremosphaera viridis* is reasonably higher (by a factor of 5–10 [26]) than the diffusional P_d values described here.

So far the studies refer to an experimental set-up where the $H_2O/^2H_2O$-exchange is directly measured at a single spot of 35 μm diameter just outside (control) or within the cell. However, the experiments can be carried on one step further using video-camera systems with extended NIR-sensitivity. This leads to two-dimensional $H_2O/^2H_2O$-exchange maps with a spatial resolution in the order of the wavelength chosen. First studies with a NIR camera revealed a fast brightening of the background following the mixing event due to the $H_2O/^2H_2O$-exchange. With a short time-delay a gradual brightening of the cyto-

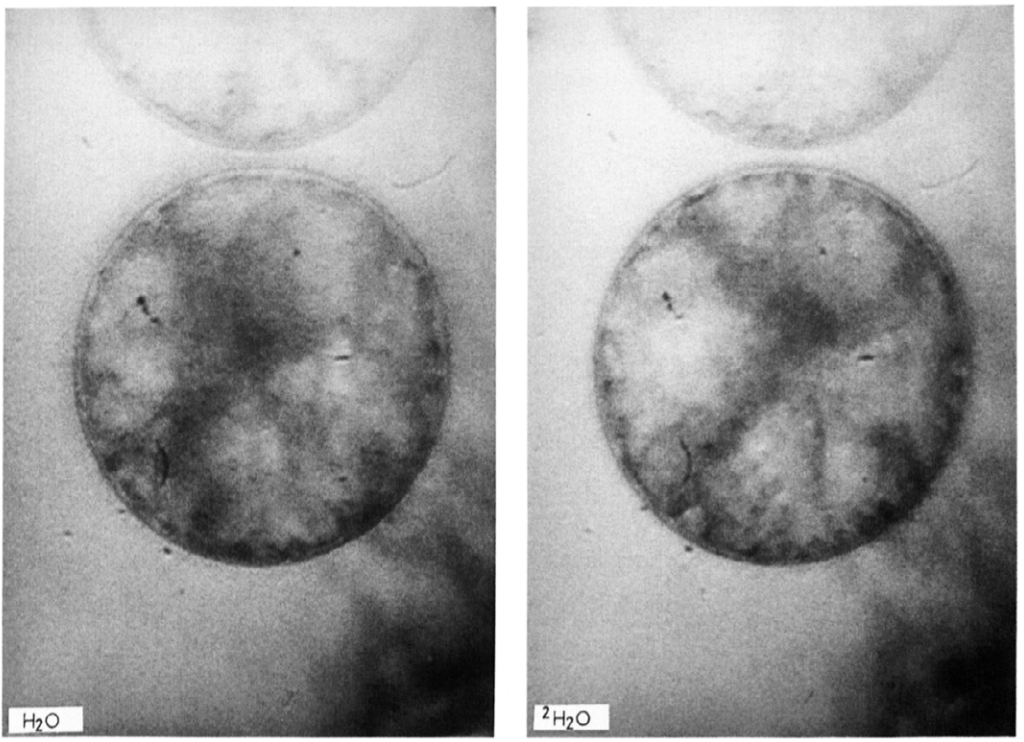

Fig. 5. Two micro-photographs of the single cell alga *Eremosphaera viridis* observed at 1450 nm with the Hamamatsu microscope video system C2400 (infrared vidicon) mounted on the Zeiss UEM microscope. The two photos show the same alga in the normal (H_2O) (left) and some seconds later in the deuterated (^2H_2O) buffer (right), respectively. Except for the isotopic solvent change all settings were equal. The diameter of the cell is 150 μm.

sol/vacuole area and of the intracellular particles was noticed. In the case of the reverse mixing experiments ($^2H_2O/H_2O$) a consecutive darkening took place. These experiments are at the beginning and Fig. 5 documents the potential of the method for the two extreme cases, i.e. the same alga in normal (H_2O) and some seconds later in deuterated buffer. Fig. 5 further reveals the cellular architecture with the radial distribution of the cytosol cords containing the chloroplasts. The results obtained so far are promising and it is hoped to get further insight into transport processes across cells, organized systems and tissues using image processing devices combined with the isotope absorption difference spectroscopy (IADS) described above. The comparably long relaxation times of the water protons seem to be a major obstacle for equivalent studies of fast exchange images by NMR microscopy.

Support from the Deutsche Forschungsgemeinschaft (SFB 176 B1) and the Fonds der Chemischen Industrie is highly acknowledged. I thank Dr. K. Köhler (Institute of Botany, University of Würzburg) for making the algae *Eremosphaera viridis* available for the present studies and for his advice. I further thank B. Lohmüller (Hamamatsu Photonics Europe, Herrsching, F.R.G.) for the experiments with the NIR-sensitive camera system.

References

1 Inoue, S. (1986) Video Microscopy. Plenum Press, New York.

2 Tsien, R.Y. (1980) Biochemistry 19, 2396–2404.
3 Ilsley, N.P. and Verkman, A.S. (1987) Biochemistry 26, 1215–1219.
4 Aguayo, J.B., Blackband, S.J., Schoeniger, J., Mattingly, M.A. and Hintermann, M. (1986) Nature 322, 190–191.
5 Hirth, U.-A. and Lawaczeck, R. (1986) Z. Naturforsch. 41c, 923–927.
6 Luck, W.A.P. (1974) in Structure of Water and Aqueous Solutions (Luck, W.A.P., ed.), pp. 247–284, Verlag Chemie, Weinheim.
7 Köhler, K., Geiswind, H.-J., Simonis, W. and Urbach, W. (1983) Planta 159, 165–171.
8 Lawaczeck, R. (1987) in Interaction of Water in Ionic and Nonionic Hydrates (Kleeberg, H., ed.), pp. 209–212, Springer-Verlag, Berlin.
9 Finkelstein, A. (1987) Water Movement Through Lipid Bilayer, Pores, and Plasma Membranes. John Wiley & Sons, New York.
10 Stein, W.D. (1986) Transport and Diffusion across Cell Membranes, Academic Press, Inc., Orlando.
11 Lawaczeck, R. (1988) in Water Transport in Biological Membranes, Vol. 1, (Benga, G. ed.), Chapter 5, CRC Press, Inc., Boca Raton, in press.
12 Weidinger, M. and Rüppel, H.G. (1985) Protoplasma 124, 184–187.
13 Longsworth, L.G. (1960) J. Phys. Chem. 64, 1914–1917.
14 Crank, J. (1964) The Mathematics of Diffusion, Oxford University Press, London.
15 Lövtrup, S. (1963) J. Theoret. Biol. 5, 341–359.
16 Fenichel, R. and Horowitz, S.B. (1969) Intracellular Transport in Biological Membranes (Dowben, R.M., ed.), pp. 177–221, Little, Brown and Company, Boston.
17 Mild, K.-H. and Lövtrup, S. (1985) Biochim. Biophys. Acta 822, 155–167.
18 Seitz, P.K., Chang, D.C., Hazlewood, C.F., Rorschach, H.E. and Clegg, J.S. (1981) Arch. Biochem. Biophys. 210, 517–524.
19 Tanner, J.E. (1983) Arch. Biochem. Biophys. 224, 416–428.
20 Ratkovic, S. and Basic, G. (1980) Bioelectrochemistry and Bioenergetics 7, 405–412.
21 Sharp, R.R. and Yocum, C.F. (1980) Biochim. Biophys. Acta 592, 169–184.
22 McCain, D.C. and Markley, J.-L. (1985) FEBS Lett. 183, 353–358.
23 Solomon, A.K. (1986) J. Membr. Biol. 94, 227–232.
24 Galey, W.R. and Brahm, J. (1985) Biochim. Biophys. Acta 818, 425–428.
25 Lawaczeck, R. (1979) J. Membr. Biol. 51, 229–261.
26 Frey, N., Büchner, K.-H. and Zimmermann, U. (1988) J. Membr. Biol. 101, 151–163.